

Published in final edited form as:

*Space Sci Rev.* 2018 February ; 214(1): .

## Retrieval of Lower Thermospheric Temperatures from O<sub>2</sub> A Band Emission: The MIGHTI Experiment on ICON

Michael H. Stevens<sup>1</sup>, Christoph R. Englert<sup>1</sup>, John M. Harlander<sup>2</sup>, Scott L. England<sup>3</sup>, Kenneth D. Marr<sup>1</sup>, Charles M. Brown<sup>1</sup>, and Thomas J. Immel<sup>4</sup>

<sup>1</sup>U.S. Naval Research Laboratory, Washington DC 20275

<sup>2</sup>Space Systems Research Corporation, Alexandria, VA 22314

<sup>3</sup>Department of Aerospace and Ocean Engineering, Virginia Polytechnic Institute and State University, Blacksburg, VA, 24061

<sup>4</sup>Space Sciences Laboratory, University of California-Berkeley, Berkeley, CA

### Abstract

The Michelson Interferometer for Global High-resolution Thermospheric Imaging (MIGHTI) is a satellite experiment scheduled to launch on NASA's Ionospheric Connection Explorer (ICON) in 2017. MIGHTI is designed to measure horizontal neutral winds and neutral temperatures in the terrestrial thermosphere. Temperatures will be inferred by imaging the molecular oxygen Atmospheric band (A band) on the limb in the lower thermosphere. MIGHTI will measure the spectral shape of the A band using discrete wavelength channels to infer the ambient temperature from the rotational envelope of the band. Here we present simulated temperature retrievals based on the as-built characteristics of the instrument and the expected emission rate profile of the A band for typical daytime and nighttime conditions. We find that for a spherically symmetric atmosphere, the measurement precision is 1 K between 90-105 km during the daytime whereas during the nighttime it increases from 1 K at 90 km to 3 K at 105 km. We also find that the accuracy is 2 K to 11 K for the same altitudes. The expected MIGHTI temperature precision is within the measurement requirements for the ICON mission.

### 1. Introduction

The measurement of temperature and its variability in the Earth's upper atmosphere provides a means to quantify both the energy delivered by the sun as well as the dominant physical and chemical processes in the atmosphere. Satellite borne measurements are particularly valuable in quantifying temperature variability with latitude, longitude, altitude, and local time (LT) on a variety of temporal and spatial scales. Simultaneously separating all of these contributions throughout the upper atmosphere continues to challenge aeronomers and new satellite observations to this end will significantly advance our understanding of how solar and lower atmospheric processes couple to the ionosphere and thermosphere.

NASA's Ionospheric Connection Explorer (ICON) is a mission designed to understand the physical connection between the upper atmosphere and the space environment. ICON is scheduled to launch in 2017 into a 575 km circular orbit with an inclination of 27° [Immel *et*

*al.*, 2018]. Among the complement of instruments aboard ICON is the Michelson Interferometer for Global High-resolution Thermospheric Imaging (MIGHTI), which is designed to measure horizontal neutral wind velocity and neutral temperature profiles [Englert *et al.*, 2017]. MIGHTI measures temperatures by observing emission from the A band of molecular oxygen ( $O_2$ ) on the limb between 90-140 km altitude.

Here we present the measurement approach and retrieval for the MIGHTI temperature product between 90-105 km, which are the primary altitudes required for the ICON science objectives [Immel *et al.*, 2018]. We outline the retrieval algorithm and quantify the uncertainties given the as-built MIGHTI specifications.

## 2. Motivation and Previous Work

One of the brightest emission features in the Earth's upper atmosphere is the  $O_2$  b  $^1\Sigma_g^+(0) - X$   $^3\Sigma_g^-(0)$  A band near 760 nm [Noxon, 1968]. The band is excited through collision with  $O(^1D)$ , resonance fluorescence or a 2-step chemical reaction involving atomic oxygen called the Barth process [Bucholtz *et al.*, 1986; Sheese *et al.*, 2010]. Peak measured limb radiances for the A band are about 10 MR near 85 km tangent altitude [Tarasick and Evans, 1993; Christensen *et al.*, 2012]. Such bright emissions allow for the retrieval of neutral temperature from the rotational envelope of the band [Skinner and Hays, 1985; Sheese *et al.*, 2010; Christensen *et al.*, 2013]. Figure 1 shows representative A band volume emission rate profiles for daytime and nighttime conditions. The daytime profile has an exponential dependence with altitude based on simulations by Yee *et al.* [2012] and satellite limb measurements reported by Christensen *et al.* [2012]. The nighttime profile is taken from that reported by Liu [2006]. We use the profiles in Figure 1 as inputs to our simulated temperature retrieval.

One important Science Objective for ICON is to determine how large-scale atmospheric waves such as nonmigrating tides control the ionosphere at low latitudes [Immel *et al.*, 2018]. This will be done using measurements of wind and temperature versus altitude, LT and geographic location. ICON's low inclination orbit allows MIGHTI to measure temperatures near the equator throughout the diurnal cycle. Typical tidal amplitudes in the lower thermosphere at low latitudes are about 25 K [England *et al.*, 2009] which drives the 12 K temperature precision requirement for MIGHTI between 90-105 km altitude [Immel *et al.*, 2018]. The MIGHTI observations will be at 5 km vertical and 500 km horizontal resolution and quantify the seasonal evolution of these important global-scale oscillations in the lower thermosphere.

## 3. Observational Approach

The  $O_2$  A band is characterized by two R branches and two P branches [Babcock and Herzberg, 1948]. The rotational lines for the two R branches and the two P branches have very small spacing [*e.g.* Ritter and Wilkerson, 1987] so that when observed at lower spectral resolution there appears to be only one R branch and one P branch. We obtain the rotational distribution of the bright (0,0) band and its temperature dependence from the HITRAN2012 database [Rothman *et al.*, 2013]. We then convolve the rotational structure of the band for a

variety of temperatures relevant to the lower thermosphere using an instrument function that is consistent with MIGHTI. We use a Hann function with a full-width at half-maximum of 2 nm and show the results in Figure 2. We will discuss the MIGHTI instrument function in greater detail later.

MIGHTI measures the A band on the limb between about 90-140 km using two virtually identical optical sensors: MIGHTI A (“Ahead”) and MIGHTI B (“Behind”). This observational approach is driven by the wind measurement, where the two optical sensors will measure the same tangent point with perpendicular lines of sight seven minutes apart to obtain both components of the horizontal wind vectors [Englert *et al.*, 2017]. These operations will enable us to check the self-consistency of the MIGHTI temperature measurement, allowing for independent and near simultaneous observations of the same tangent point from different lines of sight.

MIGHTI samples the A band spectral region at five different wavelengths in order to both measure the shape of the band and to specify a background radiance that is subtracted from the signal [Englert *et al.*, 2017]. The wavelengths of the filter passbands are selected to maximize the sensitivity to lower thermospheric temperature variations. Two filter channels sample either end of the band to define a background (754.1 nm and 780.1 nm) and three more sample its shape (760.0 nm, 762.8 nm and 765.2 nm; see Figure 2). Using three filters that sample the band shape allows the simultaneous retrieval of the atmospheric temperature and common shifts in the center wavelengths of the pass bands due to temperature drifts of the filters.

The spectral shape of the pass band for each of the MIGHTI filters is crucial for retrieving accurate temperature profiles. It is particularly important that the pass bands are properly normalized with respect to each other because it is their relative intensity that enables the determination of temperature. These pass bands were measured under expected on orbit conditions for each binned detector pixel during MIGHTI calibration [Englert *et al.*, 2017] and the sensitivity for each of the five filter channels versus wavelength and altitude is shown in Figure 3. The data shown represents the sensitivity for each altitude, obtained by averaging the respective binned pixels behind each filter for each altitude. Figure 3 illustrates that the 2 nm width used to smooth the A band signal in Figure 2 is accurate. We separately measured pass bands for the MIGHTI A and MIGHTI B optical sensors as well as nighttime and daytime measurement configurations and found similar widths as those shown in Figure 3. Nominal operations will image the A band between 90-140 km in 2.5 km altitude increments.

#### 4. Temperature Retrieval: Methodology

Using the input temperature profile in Figure 4a from NRLMSISE-00 [Picone *et al.*, 2002], we calculate limb radiance profiles for the three filters sampling the A band and show the results in Figure 4b. The relative variation of these radiance profiles with altitude allows for the determination of lower thermospheric temperatures.

We simulate the A band limb radiance observations by including the étendue of the instrument for each 2.5 km altitude increment [Englert *et al.*, 2017] and the integration time for each image (30 s and 60 s for daytime and nighttime, respectively). The optical efficiency for the MIGHTI A band channels is derived from the measured properties of the optical components and is found to be 6.82%. The contributions to the limb observation in Figure 4b are explicitly calculated for each path increment along the line-of-sight for the temperature profile shown in Figure 4a. We then add detector dark signal and an estimate for scattered light contributions based on previous A band limb observations by the Optical Spectrograph and Infrared Imaging System on the Odin satellite [Sheese *et al.*, 2010]. The contributions to this background signal are discussed further in Section 6. Statistical noise is also added based on the expected photon shot noise and the detector read noise (Figure 4b).

Using this forward model approach, we invert the line-of-sight radiances to obtain a temperature profile as a function of altitude by employing a standard Abel inversion. This approach implicitly assumes that the limb emission is spherically symmetric about the Earth's center. There is no smoothing constraint or a priori assumption for the inversion so that the temperature profile is retrieved directly from the observations. A well constrained retrieval returns a solution that is very close to the input temperature profile in Figure 4a. Multiple retrievals are obtained in this way using a Monte Carlo approach and we obtain both average retrieved temperature profile (TRETR) and an altitude dependent temperature precision from the standard deviation of the retrieved profiles.

The temperature retrieval at a given altitude is informed by the observations at higher altitudes, since the near and far field signals on the limb are required to retrieve information from the tangent altitude. MIGHTI does not sample above 140 km, where the A band can still emit during the day [Tarasick and Evans, 1993; Christensen *et al.*, 2012]. Thus, the retrieval uses the approximation of Brasseur and Solomon [1986] to quantify the emission profile at altitudes above 140 km, which requires a representative scale height for the emission above this top altitude. The nominal retrieval uses an emission scale height of 30 km at 140 km, consistent with previous observations of the A band at these altitudes [Tarasick and Evans, 1993; Christensen *et al.*, 2012; Yee *et al.*, 2012].

## 5. Temperature Retrieval: Results

Figure 5a shows the input (“ $T_{\text{TRUE}}$ ”) temperature profile used in the simulations as well as the average retrieved solution (“ $T_{\text{RETR}}$ ”). The average retrieved solution is calculated from a sufficient number of iterations for which different simulations with equal statistical properties are randomly added to the daytime limb radiance profiles (Figure 4b). We determined that 50 iterations were more than sufficient to determine a consistent average temperature and standard deviation from a daytime limb profile. Figure 5b shows the average difference between these two profiles over all iterations, indicating any inherent bias to the retrieval. Figure 5b also shows the range of solutions resulting from an emission scale height at 140 km that is a factor of two smaller and larger than the 30 km that we assume. There is a bias introduced to the daytime retrieval between 90-105 km that is between 2 K and 11 K, primarily due to the lack of knowledge on the radiance profile above 140 km.

Figure 5b also shows the difference between the input profile and the average retrieved profile for a nighttime retrieval, where the integration time is 60 s and uncertainties are similarly propagated for those conditions. We use a scale height of 5 km at the top of the nighttime profile but because of the low signals above 105 km (Figure 1), the retrievals are insensitive to this value.

Figure 6a shows the average of 50 retrieved temperature profiles and the precision of the daytime retrieval overplotted. The precision is calculated by taking the standard deviation of the ensemble of retrieved profiles at each altitude. Figure 6b shows the magnitude of this precision as a function of altitude for both daytime and nighttime retrievals. The daytime precision is 1 K between 90-105 km and increases steadily to about 6 K near 130 km. The daytime precision between 90-105 km is insensitive to assumptions about the emission scale height above the imaged altitude region. The signal is weaker for nighttime conditions (Figure 1), so although the precision is near 1 K at 90 km it increases to 3 K at 105 km where the A band emission is weaker. As discussed earlier, the three channels used in the measurement of the A band shape enable the simultaneous determination of a common wavelength shift of the filter pass bands, which could be caused by a common filter temperature change. This is because the three signal channels provide redundant information on the band shape so that the wavelength registration of the band can be simultaneously constrained. We find that for the reported altitude region between 90-105 km the wavelength shift can be determined to 0.02 nm, which corresponds to a filter temperature change of about 6 K.

## 6. Discussion

One possible source of bias in the temperature retrieval is the assumption of spherical symmetry for the atmosphere. When retrieving vertical profiles in a limb viewing geometry, this assumption is typically used so that contributions to the signal above the tangent altitude and along the line of sight can be quantified. To assess the impact of this assumption, we extracted temperatures from a general circulation model that simulates the expected upper atmospheric temperature variations [Roble and Ridley, 1994; Roble, 1996] and calculated the variation of temperature along a typical line of sight for MIGHTI. We then retrieved the temperature at the tangent point by using the model temperature for each path increment and compared that to the temperature profile at the tangent point. We find that the retrieved temperature profile varies from the profile at the tangent point by an average of 3 K for the primary science altitudes. On-orbit operations will help to quantify this bias, allowing for the retrieval of temperature at nearly the same tangent point from two different look directions (MIGHTI “A” and “B”) seven minutes apart.

The relative calibration of the three channels measured (Figures 3 and 4) is important to accurately infer the temperatures. Our laboratory data indicate that the relative calibration is known to better than 1%. To quantify the impact of this on the temperature retrievals we scaled the signal for the band at 762.8 nm by 1% and retrieved temperatures in the same way. We find that a 1% bias in the relative calibration between channels introduces only a 1-2 K bias in the temperature retrieval for altitudes between 90-105 km. The temperature

bias introduced by this uncertainty responds linearly to small variations in the relative calibration. The temperature precision is unaffected by this uncertainty.

Sheese *et al.* [2010] reported that the absorption of A band emission from altitudes below 90 km can possibly affect the A band signal measured at and above this altitude. Thus, even though MIGHTI measures a background signal at two wavelengths on either side of the A band, the band itself could sit in a well of self-absorbed attenuated light. This attenuation could either be due to the contribution of off-axis light when observing the limb or from a Rayleigh background within the field of view that is multiply scattered from lower altitudes, entering the instrument directly from altitudes at or above the tangent point.

We simulated the multiply scattered Rayleigh background at A band wavelengths using the MODTRAN spectral resolution radiative transfer model [Berk *et al.*, 2006] for the tangent altitudes relevant to the MIGHTI observations. We find that the Rayleigh background at 100 km tangent altitude is only  $\sim 10$  R and that the attenuation of the multiply scattered signal is  $\sim 1$  R. This is much less than the signal within the pass bands measured by MIGHTI (Figure 4b) and negligible in the retrieval of temperature. Therefore, in the absence of a significant component of off-axis light we can neglect the effect of this process on the MIGHTI temperature retrievals. Our estimates of the off-axis contribution when observing tangent altitudes between 90-105 km are based on the MIGHTI baffle performance that was quantitatively determined using the as-built design [Englert *et al.*, 2017]. We will verify and, if necessary, correct the contribution to the limb radiance from off-axis light [Sheese *et al.*, 2010] using the background channels while on orbit by assessing the altitude dependence of the background brightness profile.

Slanger *et al.* [2017] recently reported that the  $N_2$  first positive group (1PG)  $B^3\Pi(3) - A^3\Sigma(1)$  band near 762.7 nm can contribute to  $O_2$  A band emission observations and affect the retrieval of temperature. We determined its potential contribution by using the  $N_2$  1PG dayglow system limb intensity reported by Broadfoot *et al.* [1997] of 200 kR at 140 km. The relative intensity of the  $N_2$  1PG (3,1) band is 7.2% as given by Vallance Jones [1974], so that the estimated (3,1) limb intensity is 14 kR at 140 km. If applied entirely to the 762.8 nm MIGHTI channel at all altitudes at and below 140 km, this can bias temperatures by  $\sim 10$  K near 140 km but in the region of primary science between 90-105 km the A band signal is much larger (see Figure 1) and the estimated bias is less than 2 K.

## 7. Summary

We have modeled the retrieval of temperature from the Earth's lower thermosphere using simulated MIGHTI observations of the  $O_2$  A band. Using our best estimates of instrument performance, we find that the precision of a daytime retrieval is about 1 K between 90-105 km for one daytime image, obtained at a cadence of 30 s. The precision of a nighttime image is about 1 K at 90 km and increases to 3 K at 105 km, obtained at a cadence of 60 s. Systematic uncertainties are between 2 K and 11 K between 95-105 km. The simplifying assumption of a spherically symmetric atmosphere contributes an additional 3 K bias to the retrieval. Redundant information in the temperature channels will allow us to constrain any

common thermal filter drift affecting the center wavelengths of the pass bands to within 0.02 nm for these same altitudes.

The expected temperature precision is well within the 12 K minimum requirement for the ICON mission. Therefore, the MIGHTI A band temperature measurement will quantitatively advance our understanding of large-scale waves in the low latitude thermosphere.

## Acknowledgments

ICON is supported by NASA's Explorers Program through contracts NNG12FA45C and NNG12FA421.

## References

- Babcock HD, Herzberg L. *Ap J*. 1948; 108:167.
- Berk A, et al. *Proc SPIE*. 2006; 6233:623331F.
- Brasseur G, Solomon S. *Aeronomy of the Middle Atmosphere*. 2nd. D. Reidel; Dordrecht: 1986. 107
- Broadfoot AL, et al. *J Geophys Res*. 1997; 102:11,567.
- Bucholtz A, et al. *Planet Space Sci*. 1986; 34:1031.
- Christensen AB, et al. *J Geophys Res*. 2012; doi: 10.1029/2011JA016838
- Christensen AB, et al. *J Geophys Res*. 2013; doi: 10.1002/jgra.50317
- England SL, et al. *Earth Planets Space*. 2009; 61:493.
- Englert CR, et al. *Space Sci Rev*. 2017; doi: 10.1007/s11214-017-0358-4
- Immel TJ, , et al. *Space Sci Rev*. 2018.
- Liu G. PhD Dissertation. York University; Toronto, Ontario, Canada: 2006.
- Noxon JF. *Space Sci Rev*. 1968; 8:92.
- Picone JM, et al. *J Geophys Res*. 2002; doi: 10.1029/2002JA009430
- Ritter KJ, Wilkerson TD. *J Mol Spect*. 1987; 121:1.
- Roble RG, Schunk R, editors *STEP Handbook on Ionospheric Models*. Utah State Univ; Logan: 1996. 281
- Roble RG, Ridley EC. *Geophys Res Lett*. 1994; doi: 10.1029/93GL03391
- Rothman LS, et al. *JQSRT*. 2013; 130:4.
- Sheese PE, et al. *Can J Phys*. 2010; 88:919.
- Skinner WR, Hays PB. *Appl Opt*. 1985; 25:4272.
- Slanger TG, et al. *J Geophys Res*. 2017; 122:3640.doi: 10.1002/2016JA023502
- Tarasick DW, Evans WFJ. *Adv Space Res*. 1993; 13:145.
- Jones A Vallance. *Aurora, Geophys And Astrophys Monogr Ser*. Vol. 9. D. Reidel; 1974.
- Yee JH, et al. *Can J Phys*. 2012; 90:769.

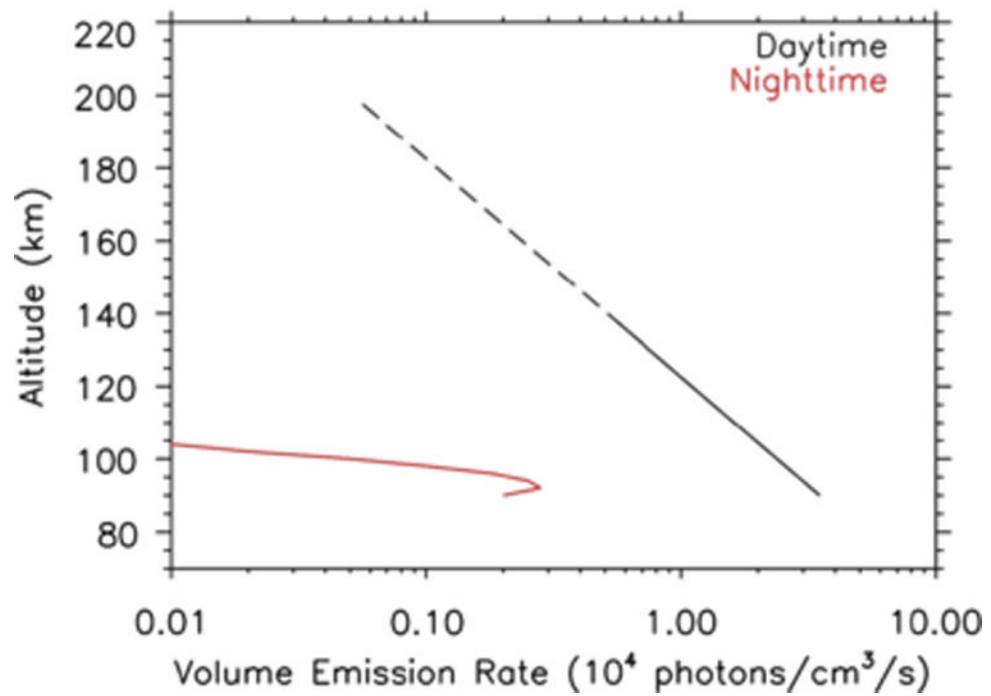


**Figure 1.**  $O_2$  (0,0) A band volume emission rate profiles used to retrieve temperatures for daytime [black; fit to results of Christensen *et al.*, 2012] and nighttime [red; Liu, 2006]. The altitudes shown by the dashed line will not be observed operationally by MIGHTI.



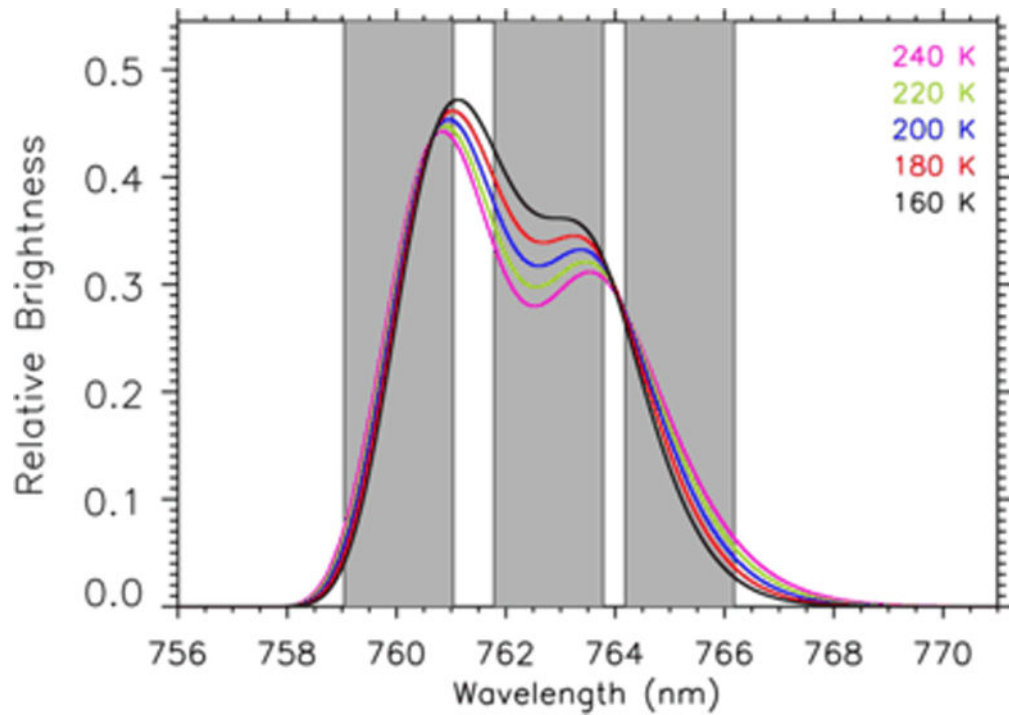


**Figure 2.**

The  $O_2$  (0,0) A band at a variety of temperatures relevant to the Earth's lower thermosphere [Rothman *et al.*, 2013]. The rotational structure has been smoothed by the MIGHTI pass band with a full-width at half-maximum of 2 nm. The three shaded areas represent the (4 nm) spectral regions that are selected for greatest sensitivity to the lower thermospheric variation in the band shape.

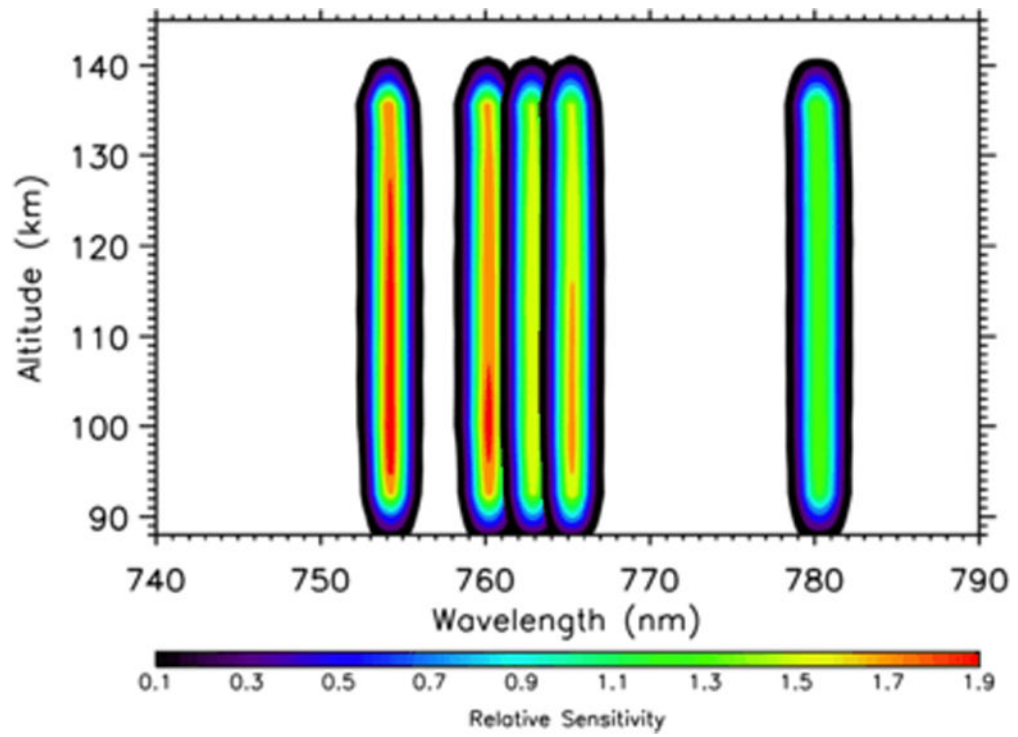


**Figure 3.**

The relative sensitivity of the five MIGHTI A pass bands used in this study for the daytime A (Ahead) optical sensor. The two pass bands on either end are used to determine the background to subtract from the three middle pass bands which overlap the A band.

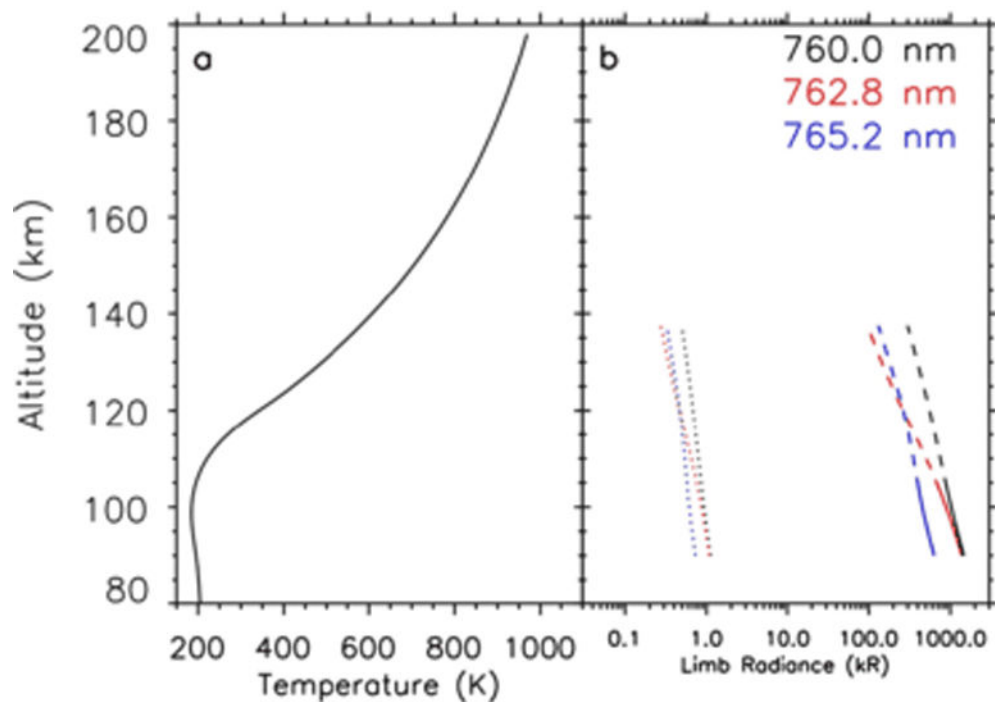


**Figure 4.**

(a) Representative temperature profile used in this study, from NRLMSISE-00 sampled on 1 April at 2.5° S and 12 LT [Picone *et al.*, 2002]. (b) Calculated limb radiances for the three pass bands centered at the indicated A band wavelengths, along with the expected statistical uncertainty for each channel (dotted lines). Although MIGHTI images to the top of the region indicated by the dashed lines, the primary science region at lower altitudes (90-105 km) is indicated with solid lines. The ratios of these three limb radiance profiles with altitude are diagnostic of the temperature profile shown in Figure 4a.

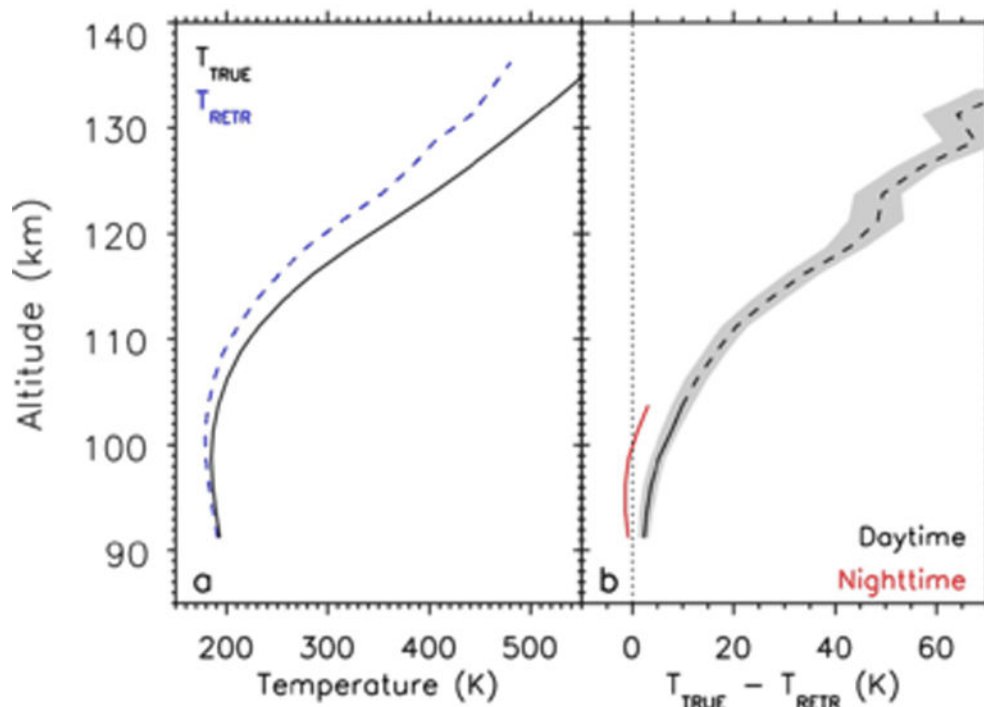


**Figure 5.**

(a) True temperature profile ( $T_{TRUE}$ , solid) and average retrieved daytime temperature profile ( $T_{RETR}$ , dashed) from 50 simulated retrievals. (b) The difference between the true profile and the average retrieved profile. The altitudes shown by the black solid line (90-105 km) represent the region of primary MIGHTI science. The red line shows the result for a nighttime retrieval. The shaded area represents variations resulting from changes in the assumed 30 km emission scale height at 140 km of a factor of two more and less.

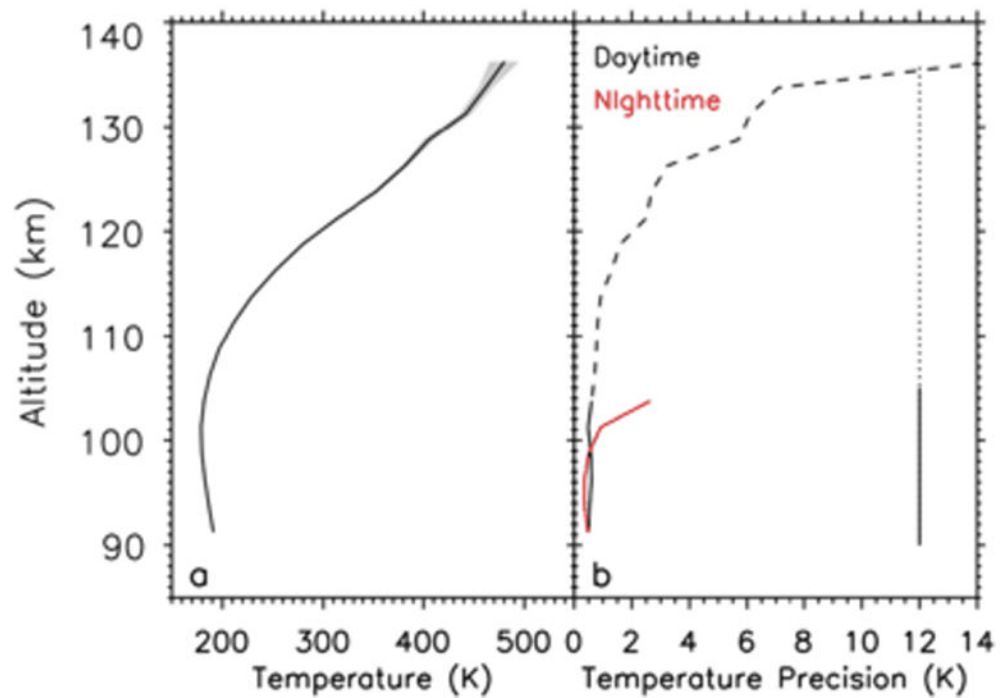


**Figure 6.**

(a) Averaged retrieved daytime temperature with estimated 1- $\sigma$  uncertainty overplotted as the shaded area. The uncertainties are calculated as the standard deviation of the average over all simulations. (b) The average 1- $\sigma$  uncertainty (temperature precision) shown in Figure 6a. The altitudes shown by the solid line (90-105 km) represent the region of primary MIGHTI science. The red line shows the result for a nighttime retrieval. The vertical line at 12 K shows the precision required between 90-105 km (solid) and extended to higher altitudes (dotted).